







Document Approval:
Date Approved

Originator: Zhirong Huang, Physicist		1/13/2015
Approver: Paul Emma, System Physicist		1/14/15
Approver: Ginger DeContreras, Injector Control Account Manager		1/14/2015
Approver: Jose Chan, Accelerator System Manager		1/14/15
Approver: David Schultz, Project Technical Director		1-14-15
Approver: Tor Raubenheimer, Physics Team Lead		1/14/15

Revision History

Revision	Date Released	Description of Change
R1	1/14/2015	Changes since CDR: Longer heater chicane with smaller R56 to reduce micro-bunching (R56 was -14 mm and now is -3.5 mm)
R0	4/7/2014	Original Release.

1 Purpose

This document describes physics principles and requirements for the laser heater subsystem of the LCLS-II injector.

2 Scope
3 Definitions

LH	Laser Heater
----	--------------

4 References

[1]	Marco Venturini, Z. Huang, <i>Laser heater: scaling of laser power with undulator period and laser wavelength</i> , LCLS-II-TN-14-05, 2014.
-----	---

5 Responsibilities

Zhirong Huang	Physicist
Paul Emma	System Physicist
Ginger DeContreras	Injector Control Account Manager
Jose Chan	Accelerator System Manager

6 Overview - Document Content

The LCLS-II injector system will incorporate a laser-electron-beam heater system (an inverse free electron laser) in order to generate an uncorrelated energy spread in the electron beam. This produces Landau damping in the bunch compressor chicanes in order to suppress potential micro-bunching instabilities that may be driven by Coherent Synchrotron Radiation (CSR) in the bunch compressors, and Longitudinal Space Charge (LSC) forces in the linac. The laser-heater beam optics is shown in Fig. 1. The heater system is located just downstream of the L0 accelerator section at 98 MeV.

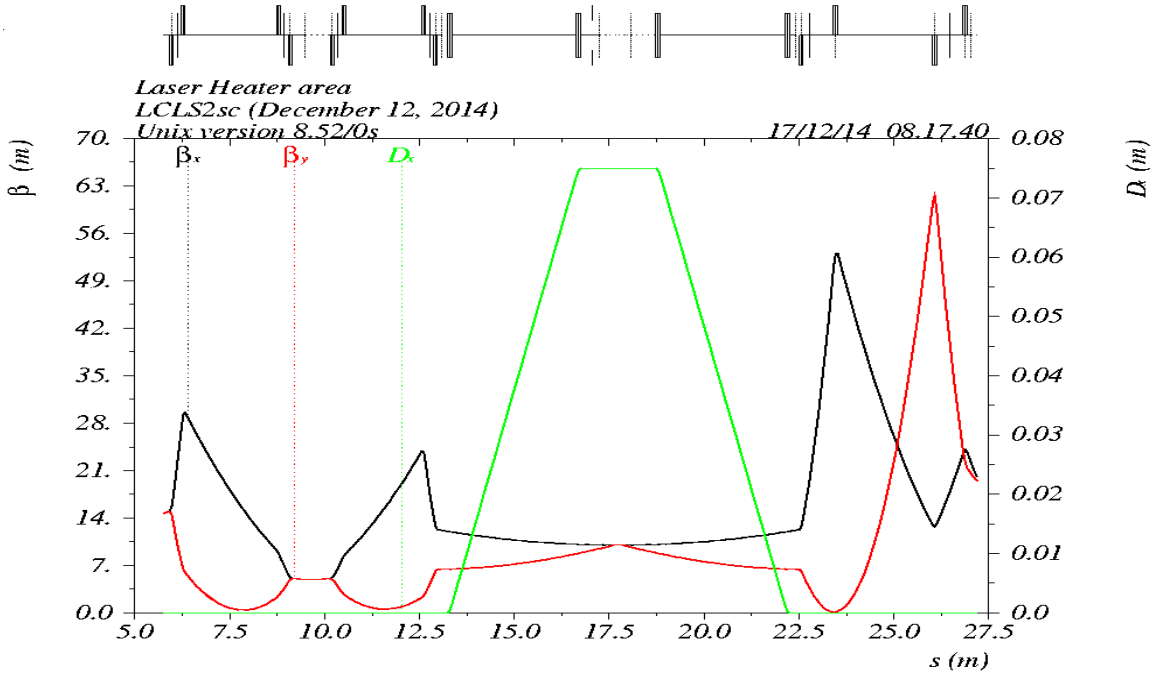


Figure 1: Beta and dispersion functions along the laser heater section from exit of CM01 module to within a few meters of the L1-linac RF section. The undulator center is at $s \approx 17.5$ m where the beta functions (β_x & β_y) are about 10 m and the hor. dispersion, D_x , is 75 mm.

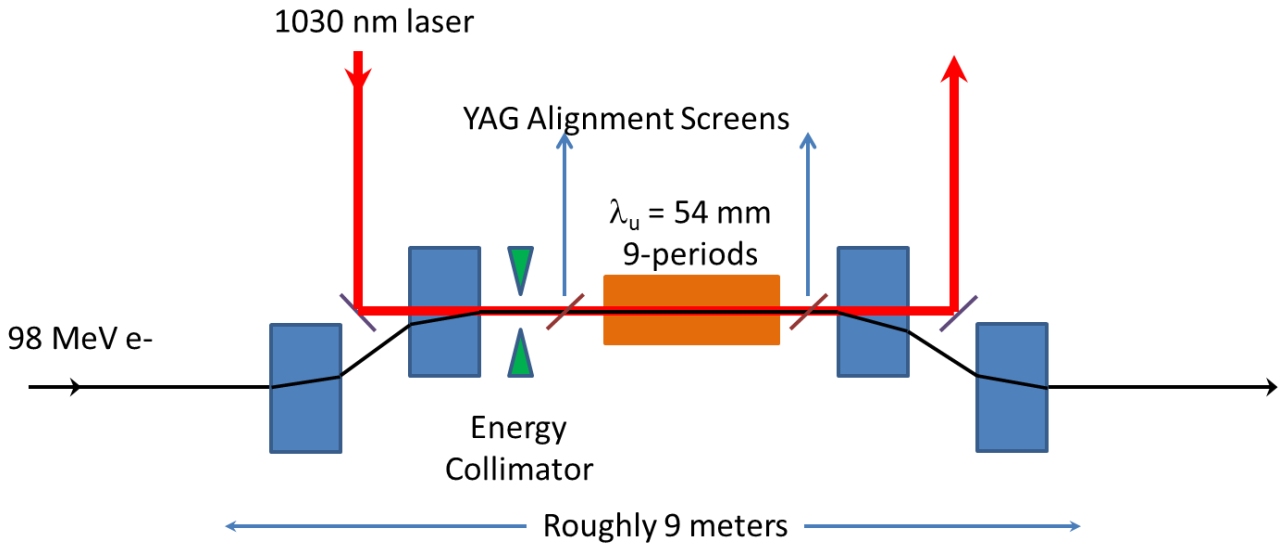


Figure 2: Schematic of the laser heater system including an energy collimation system and two pop-in screens to align the laser and the electron beam. The chicane length is roughly 9 meters.

An upper limit to the heating capacity required of the LH is set by the maximum allowable rms energy spread $\sigma_{E,FEL}$ at the FEL and total magnetic compression factor C_T . For the $Q = 100$ pC baseline beam, we have $\sigma_{E,FEL} \approx 500$ keV and $C_T \approx 85$, implying that heating from the LH should not exceed about $\sigma_{E,FEL}/C_T \approx 6$ keV rms. We believe this is sufficient to suppress the microbunching instability, although further confirmation will be needed. To leave room for other modes of machine operation, we set a $\sigma_{E,LH} = 20$ keV rms requirement for the maximum heating capacity. The laser pulse is assumed to be Gaussian, both transversely and longitudinally. The required pulse energy takes into account a 50% larger laser spot size at the middle of undulator (than the electron beam size) for easier transverse overlapping.

Our choice $\lambda = 1030$ nm for the laser wavelength is primarily dictated by the availability of high-power, high-repetition rate sources (e.g., Yb: glass fibers). We plan to use the LCLS-II phase I heater undulator with period $\lambda_u = 5.4$ cm. (Note that the undulator will be installed with a vertical magnetic field (a horizontal wiggler) and the laser must be polarized in the horizontal direction.) A moderate number $N_u = 9$ of undulator periods are selected so as to broaden the bandwidth of the undulator resonance condition to a few percent. The resonance requires an electron energy accuracy of about $\pm 2\%$ in order to reach 90% efficiency as calculated. The adjustable-gap heater undulator can operate at the upper end (120 MeV) of the injector beam energy range by decreasing the undulator gap ($g_{min} = 3.2$ cm) and hence increase the peak magnetic field to 0.3 T [1]. In this analysis the undulator peak magnetic field is assumed to be given by $B_0 = b \exp(-ag/\lambda_u)$, with $b = 2.08$ T and $a = 3.24$, consistent at the few percent level with the field measurements of the undulator presently installed in the LCLS LH. The nominal parameters of the laser heater system are listed in Table 1 and a sketch appears in Figure 2.

Since the injector energy can vary from 90 MeV to 120 MeV, we can maintain the resonant condition by tuning the magnetic undulator gap from 4.3 cm to 3.25 cm. The heating efficiency will increase with the undulator magnetic field. Figure 3 shows the required laser pulse energy as a function of the electron beam energy for 6 keV induced rms energy spread.

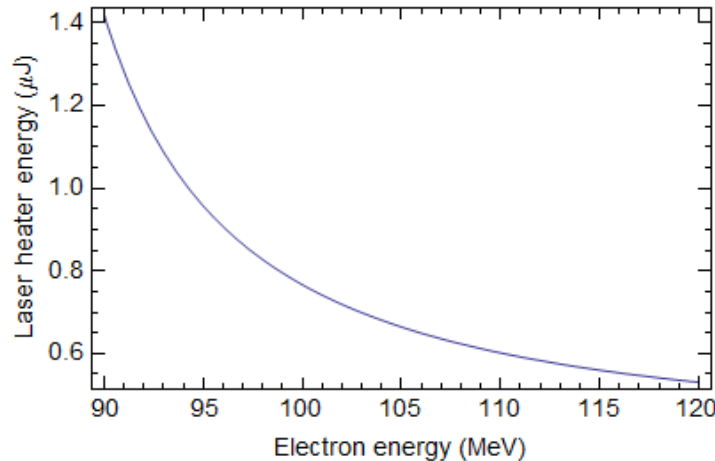


Figure 3: Laser pulse energy vs. electron beam energy for 6 keV rms energy spread induced by the laser heater (100 pC bunch case).

The laser heater system will also include two YAG screens to spatially align the electron and laser beams, an adjustable collimator located just upstream of the undulator to limit the bunch energy spread and energy deviations to $\sim \pm 3\%$, and a synchrotron radiation port for parasitic bunch energy spread diagnostics. A 3% energy deviation corresponds to 2.3 mm collimator gap which is greater than 10 times the rms beams size.

Two YAG screens are included with one on each side of the undulator. These are insertable foils with optics and cameras and will be designed to insert horizontally (or vertically), depending on mechanical layout interference issues. The YAG screens only need to intercept the beam when the chicane dipole magnets are powered, as shown in Figure 2. When extracted, the YAG screens should not intercept the electron or laser beams in any condition (dipoles on or off). The YAG screens will not be inserted at the full beam rate and will only be used at 100 Hz or less.

Each YAG optics package should include a fast photodiode with rise time less than 30 ps (including cables) in order to sense the electron arrival time using the YAG light. Another photodiode on the laser will be used to establish coincidence.

Laser diagnostics are described in detail elsewhere, but include an imaging camera, power meter, photodiode, piezo controlled mirrors for laser position feedback control, an adjustable delay line, and a fast Pockels cell and waveplate for energy control.

Table 1. Laser Heater parameters (Nominal values are taken for 100 pC bunches at 1 MHz).

Parameter	Symbol	Nominal	Range	Unit
Electron beam energy	E	98	90-120	MeV
Betatron functions (at LH undulator center)	$\beta_x = \beta_y$	10	8-12	m
Normalized transverse emittance (used in these LH calculations)	$\varepsilon_{nx} = \varepsilon_{ny}$	0.3	0.1-0.7	μm
Electron beam transverse rms sizes (at LH undulator center)	$\sigma_x = \sigma_y$	130	80-200	μm
Chicane dipole bend angles	$ \theta_B $	0.022	-	rad
Chicane dipoles lengths	L_B	0.124	-	m
Drift from 1 st -to-2 nd and 3 rd -to-4 th dipole	ΔL_1	3.28	-	m
Dispersion (at undulator)	$ D_x $	7.5	-	cm
Horizontal offset of undulator from linac axis	Δx	7.5	-	cm
Momentum compaction (over full chicane)	$ R_{56} $	3.5	-	mm
Undulator gap (minimum 3.0 cm)	g	4.1	4.3-3.20	cm
Undulator period	λ_u	5.4	-	cm
Undulator parameter	K	0.9	0.8-1.49	-
Undulator peak magnetic field	B_0	0.18	0.16-0.30	T
Number of undulator periods	N_u	9	-	-
Laser wavelength	λ	1030		nm
Laser pulse transverse rms size (middle of undulator)	σ_r	195	120-300	μm
Rayleigh length	Z_R	46	18-110	cm
Laser pulse length (FWHM)	T_L	20	10-30	ps
Beam rms-energy spread induced by Laser Heater (max.)	σ_E	6	0-20*	keV
Laser pulse energy at undulator	E_L	1	0-15	μJ
Laser pulse peak power at undulator	P_L	0.05	0-1.5	MW
Laser average power at undulator (at 1 MHz)	P_{avg}	1	0-15	W

* For 0.7- μm emittance (at 300 pC charge per bunch), a 20 keV rms energy spread can be generated by matching the laser transverse spot size with the electron transverse spot size.